RETO GIERÉ

Zirconolite, Allanite and Hoegbomite in a Marble Skarn from the Bergell Contact Aureole: Implications for Mobility of Ti, Zr and REE

Originalbeitrag erschienen in:
Contributions to mineralogy and petrology 93 (1986), S. 459 - 470

Contrib Mineral Petrol (1986) 93:459–470

Contributions to Mineralogy and Petrology

Zirconolite, allanite and hoegbomite in a marble skarn from the Bergell contact aureole: implications for mobility of Ti, Zr and REE

Reto Gieré
Institut für Mineralogie und Petrographie, ETH-Zentrum, CH-8092 Zürich, Switzerland

Abstract. Zirconolite, allanite and hoegbomite are present as accessory phases in a metasomatically altered spinel-calcite-marble from the contact with the Bergell intrusives (Switzerland/Italy). Textural relationships indicate a stepwise alteration of spinel to 1) hoegbomite or corundum + magnetite, 2) margarite and 3) chlorite. Replacement of spinel by hoegbomite can be described by the substitution $1.94(Mg^{2+}, Fe^{2+}, Zn^{2+}, Mn^{2+}, Ca^{2+}) \rightleftharpoons Ti^{4+} + 0.12(OH^-)$ where Al^{3+} and Fe^{3+} are held constant. The average composition of the Bergell hoegbomites is given by the formula $Fe^{2+}_{0.97}Mg_{0.69}Zn_{0.04}Ti_{0.17}Al_{3.94}Fe^{3+}_{0.06}O_{7.98}(OH)_{0.02}$ and seems to be imposed by the composition of pre-existing spinel. During the first two steps of spinel alteration, calcite was replaced by anorthite + phlogopite, and the rare earth element(REE)-bearing minerals zirconolite, allanite and sphene were formed. Allanites have characteristic chondrite-normalized REE patterns with enrichment in the light REE. The zirconolite patterns show a marked increase in concentration from La to Ce, followed by an almost constant section. Sphene lacks detectable La, and its REE patterns vary from grain to grain. Contemporaneous formation of phlogopite, REE-bearing minerals and hoegbomite during replacement of the spinel-calcite-marble indicates that the metamorphic fluid introduced potassium along with REE and other high valence cations (Ti^{4+}, Zr^{4+}, U^{4+}, Th^{4+}, Nb^{5+}, Y^{3+}) possibly as polynuclear complexes. The abundance of fluorine-bearing phlogopite and fluor-apatite as well as their close association with REE-bearing minerals and hoegbomite suggests F^- and PO_4^{3-} as likely ligands for complexing of the above mentioned elements.

Introduction

Zirconolite, allanite and hoegbomite have been identified as accessory minerals in a metasomatically altered spinel-calcite-marble from the eastern margin of the Tertiary Bergell calc-alkaline intrusives (Switzerland/Italy). The sample was collected from the talus at the south-eastern foot of Cima di Vazzeda (Swiss coordinates: 776.600/131.100). The direct relationship to the plutonic rocks could therefore not be studied in the field. The Cima di Vazzeda is composed of contact metamorphic gneisses and marbles, which belong to the Mesozoic cover of the upper Penninic Suretta nappe (Gieré 1985) and are crosscut by the Bergell granodiorite (Diethelm 1984, Gieré 1984). Following contact metamorphism, metasomatic processes formed symmetrically zoned reaction veins in the dolomitic marbles (Bucher-Nurminen 1981).

In this paper the mineralogy and the textural relationships observed in the metasomatically altered spinel-calcite-marble are described. Special attention is drawn to the compositions of zirconolite, allanite and hoegbomite, which have only rarely been reported from limestone skarns. Concentrations of five rare earth elements (REE) and yttrium have been determined by electron microprobe analysis in zirconolite, allanite and sphene. The chondrite-normalized REE patterns of these minerals are presented. Finally, problems concerning the genesis of REE-bearing minerals and phases rich in Ti, Zr, Th and U through metasomatic processes will be discussed.

Zirconolite, zirkelite and polymignyte have often been considered the same mineral. Recently however, Mazzi and Munno (1983) showed that the three phases were polymorphs of the same compound given by the simplified formula $CaZrTi_2O_7$ (cf. Coughanour et al. 1955). Zirconolite is monoclinic (Pyatenko and Pudovkina 1964; Rossell 1980; Gatehouse et al. 1981; Sinclair and Eggleton 1982), while zirkelite is trigonal and polymignyte is orthorhombic (Mazzi and Munno 1983).

Zirconolite has been reported from a wide variety of terrestrial rocks as well as from lunar samples, and considerable variations in composition have been observed. For simplicity, the name zirconolite is used here to describe all $CaZrTi_2O_7$-compounds referred to. There is much confusion in the literature regarding nomenclature and composition, and most of the zirconolites have not been investigated by X-ray analyses. Zirconolite is a rare mineral on earth. It occurs in mesostasis areas of ultrabasic cumulates (Williams 1978), in gabbroic pegmatites (Harding et al. 1982), in sanidinites (Mazzi and Munno 1983) and in carbonatites (Kapustin 1966; Zhuravleva et al. 1976; Sinclair and Eggleton 1982). The mineral is also known from altered pyroxenites (Hussak and Prior 1897, Borodin et al. 1956, 1961). Semenov et al. (1963) found zirconolite in fenitized country rocks around nepheline syenites, and Zhuravleva et al. (1976) reported an occurrence in metasomatically altered iron ores. Parageneses with jordisite and pyrite in hydrothermal veins have been studied by Rekharskiy and Rekharskaya (1969). It is also a constituent of heavy mineral sands from Sri Lanka (Blake and Smith 1913). Recently, an occurrence of zirconolite in marble lenses of the Oetztal, Austria, has been described by Purtscheller and Tessadri

(1985). Zirconolite is a common accessory phase in lunar samples where it crystallized from late-stage, U-enriched liquids in mesostasis areas of mare basalts (Meyer and Boctor 1974, Wark et al. 1974; Lovering and Wark 1974) as well as in feldspathic peridotites and norites (Busche et al. 1972).

Hoegbomite, a complex Fe-Mg-Al-Ti-oxide, forms a series of polytypes with hexagonal or rhombohedral lattices (McKie 1964). The mineral was first described by Gavelin (1916) in magmatic titaniferous iron ores where it was considered to be a primary phase. Since its discovery, hoegbomite has been observed in many different rock types. Its close association with green spinel is a common feature of most occurrences. Hoegbomite is a typical constituent of magnetite-spinel-corundum-assemblages in emery deposits (Watson 1925; Gillson and Kania 1930; De Lapparent 1946; Friedman 1952), where it frequently formed by spinel alteration. It is a common accessory mineral in spinel-cordierite-bearing metapelites (Leake and Skirrow 1960; Evans 1964; Woodford and Wilson 1976; Mancktelow 1981; Spry 1982; Angus and Middleton 1985). In a contact metamorphic, cordierite-free pelitic schist from the eastern Bergell, Gieré (1984) found hoegbomite, green spinel, corundum and rutile as inclusions in porphyroblastic andalusite. At Corno di Gesero, Switzerland, hoegbomite associated with green spinel occurs in a hornblende-chlorite-olivine-blackwall (Trommsdorff and Evans 1979). Hoegbomite-spinel-assemblages are further reported from titanomagnetite ores (Zakrzewski 1977), from pyroxenites (Christophe-Michel-Lévy and Sandréa 1953; Coolen 1981; Angus and Middleton 1985) and from granulite-facies metagabbros and calcsilicate rocks (Coolen 1981). Spinel-free parageneses however, have been described by Oenay (1949) in emery deposits, by McKie (1964) in magnesium-rich skarns and by Gillson and Kania (1930), Friedman (1952), Leake (1965) and Čech et al. (1976) in pelitic rocks.

Allanite, an epidote group mineral rich in REE, is a common accessory phase in granites, granodiorites, monzonites, syenites and pegmatites (see Deer et al. 1962), and occurs as phenocrysts also in acid volcanic rocks such as rhyolites (Duggan 1976) and perlitic obsidian (Brooks et al. 1981). Further, it is found in schists and gneisses (see Deer et al. 1962). Allanite as a hydrothermal mineral in rocks from Skye, Scotland, has been described by Exley (1980), who also observed it as detrital grains in the Torridonian arkoses. Metasomatically formed allanite however, has only rarely been reported: in limestone skarns by Rudashevskiy (1969) and by Pavelescu and Pavelescu (1972), in regional metamorphic calc-silicate rocks by Sargent (1964). Allanite occurs also in carbonate veins of the Mountain Pass district, California (Olson et al. 1954).

Table 1. Electron microprobe detection limits and relative errors (%) due to counting statistics (1 sigma) for the REE-bearing minerals

	Zirconolite		Allanite		Sphene	
	detection limit (ppm)	relative error (%)	detection limit (ppm)	relative error (%)	detection limit (ppm)	relative error (%)
ZrO_2	1,330	0.3	710	9.9	900	10.7
CaO	890	0.3	780	0.2	860	0.2
TiO_2	1,770	0.3	1,610	–	1,450	0.3
Al_2O_3	80	1.1	90	0.2	80	0.7
FeO	1,740	1.7	1,510	1.0	1,360	11.3
MgO	90	6.4	90	1.0	90	–
ZnO	390	10.0	310	–	310	14.8
SiO_2	110	2.0	110	0.1	110	0.1
ThO_2	140	1.9	110	2.2	110	7.1
La_2O_3	170	3.6	130	0.6	140	11.1
Ce_2O_3	330	2.5	290	1.1	330	8.0
Nd_2O_3	350	3.0	310	1.6	310	9.7
Gd_2O_3	250	3.8	200	2.4	200	11.5
Dy_2O_3	370	5.4	320	–	270	9.6
Y_2O_3	240	2.0	180	9.1	180	5.4

Analytical procedure

Analyses were performed using an automated ARL SEMQ microprobe, operated at an acceleration potential of 15 kV and a sample current of 20 nA (measured on brass), yielding a beam size of 0.2 µm. Six crystal X-ray spectrometers and an X-ray energy dispersive analyzer (TN 2000 by Tracor Northern) were applied simultaneously. Samples and standards were coated with 200 Å of carbon. Minor element standards used for quantitative analyses were synthetic oxides and glasses for REE, Zr, and Th, natural xenotime for Y and natural gahnite for Zn. In REE-bearing minerals relative errors due to counting statistics were reduced by using a data collection time of 100 seconds at each peak (Lα1 for REE). Two positions for background determination, above and below the peaks, were fixed on the basis of wavelength spectra. Detection limits and relative errors (1 sigma) for each REE-mineral are listed in Table 1. Errors for Gd and Dy might be larger due to intra-REE interferences. Table 2 shows the relative errors (1 sigma) for the

Table 2. Relative errors (%) due to counting statistics (1 sigma) for main minerals

	Spinel	Hoegbomite	Margarite	Chlorite	Phlogopite	Anorthite	Clinozoisite
Al_2O_3	0.5	0.5	0.5	0.9	1.0	0.6	0.7
TiO_2	–	3.7	23.5	22.0	5.6	–	18.9
SiO_2	–	–	0.7	0.8	0.6	0.5	0.6
MgO	1.2	1.2	5.6	0.4	0.4	–	10.8
CaO	5.3	5.3	1.0	–	–	0.8	0.7
MnO	18.0	–	–	14.5	–	–	–
FeO	1.7	1.8	5.6	1.1	1.1	9.6	1.5
ZnO	3.0	4.2	–	–	–	–	–
Na_2O	–	–	2.8	–	7.5	7.8	–
K_2O	–	–	3.0	8.0	0.4	13.2	8.7
F	–	–	–	–	17.5	–	–
Cl	–	–	16.0	15.7	15.9	21.7	15.8

analyses of all other minerals. The raw data were corrected on-line for drift, dead-time and background. Full corrections for X-ray absorption, X-ray fluorescence by characteristic and continuous excitation, atomic number effect, backscatter losses and ionisation-penetration losses were applied to the data by a ZAF computer program at the ETH Zürich.

Petrography

The hand-specimen is coarse-grained and massive. Numerous white calcite lenses with a black core are embedded in a dark groundmass consisting of anorthite + phlogopite + relictic calcite (Fig. 1). The calcite lenses (up to 2 cm in diameter) exhibit a distinct zoning with spinel, hoegbomite, corundum and magnetite in the center, and margarite or chlorite towards the margin. Between the calcite lenses and the groundmass there is either a sharp boundary or a narrow transition zone which, in addition to the matrix minerals, contains apatite and chlorite, the latter replacing phlogopite.

Calcite lenses

Calcite shows a mosaic texture. No dolomite exsolution is visible and the average calcite composition is 98.3 wt% $CaCO_3$, 1.27 wt% $MgCO_3$, 0.39 wt% $FeCO_3$, 0.03 wt% $MnCO_3$.

Spinel is dark green to black in thin section. Some spinels enclose REE-free clinozoisite which differs in composition from the matrix clinozoisite (see below). The Fe_2O_3-poor spinel contains up to 5.4 wt% ZnO and lies on the Fe-rich side of the spinel-hercynite solid solution series (Table 5). Exsolution lamellae of magnetite are present within some grains. Four different replace-

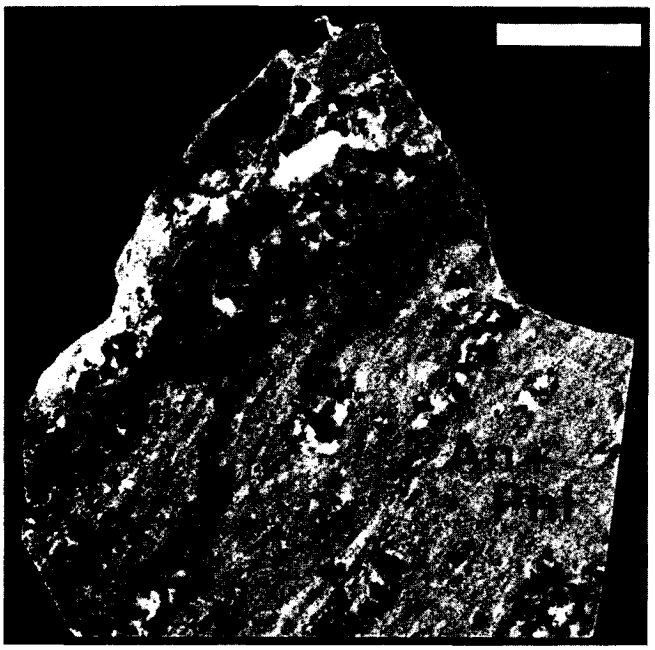

Fig. 1. Photograph of the hand specimen showing calcite lenses embedded in a matrix of anorthite (An) and phlogopite (Phl). The black core of the lenses consists mainly of spinel, hoegbomite, corundum and magnetite. Dark matrix areas contain more modal phlogopite than the bright areas. Bar is 2 cm

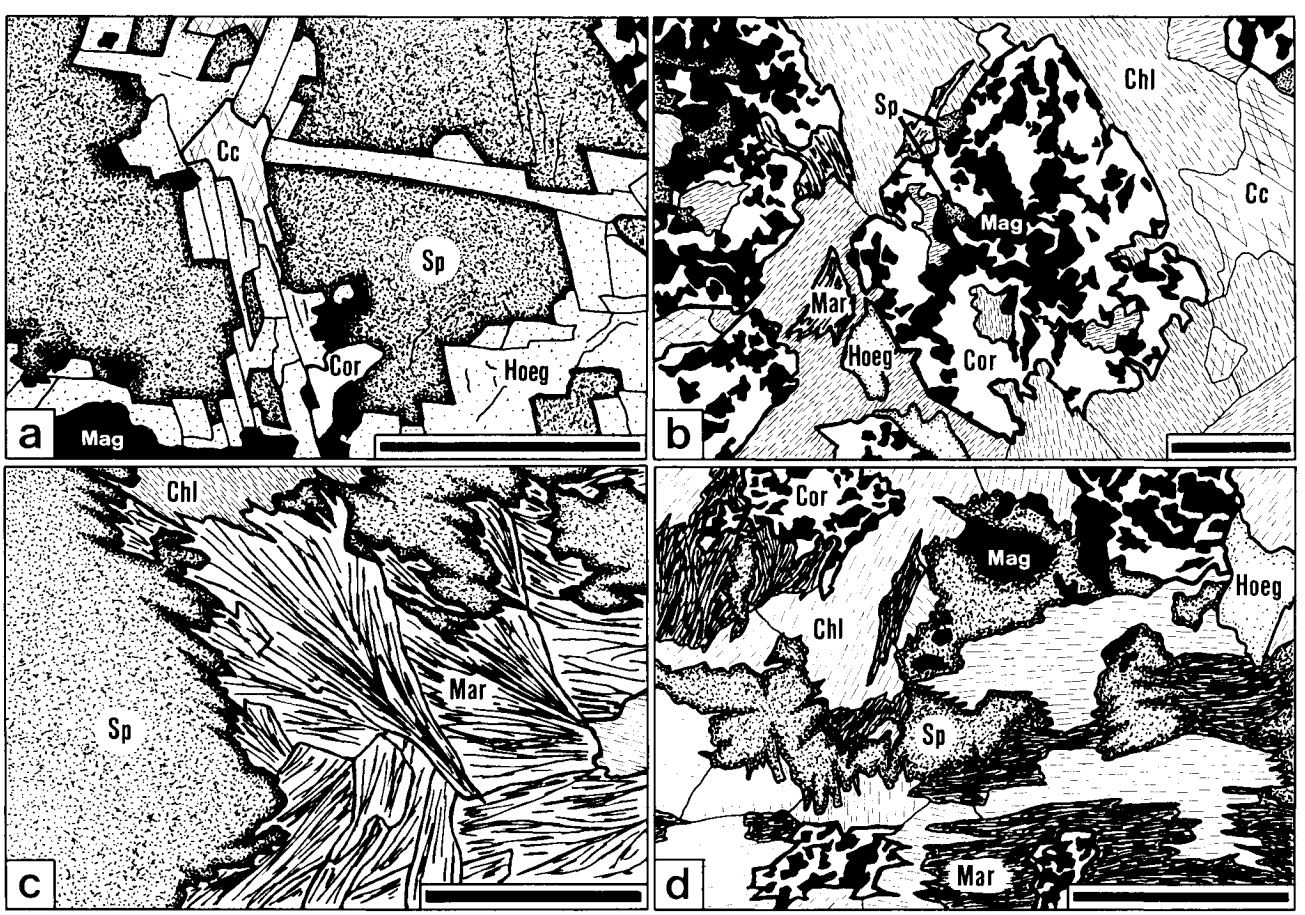

Fig. 2a–d. Drawings from thin section showing four replacement products of spinel (Sp). Bars are 0.2 mm. **a** hoegbomite (Hoeg), rimming Sp **b** corundum (Cor) + vermicular magnetite (Mag). Note Sp relic in the pseudomorph **c** margarite (Mar), overgrowing Sp **d** chlorite (Chl), overgrowing Sp

ment products of the zincian spinel can be recognized: 1) zincian hoegbomite, 2) corundum + magnetite, 3) margarite and 4) chlorite. Replacement is evident from the textures: zincian hoegbomite and corundum + magnetite form either rims around or pseudomorphs after spinel (Fig. 2a, 2b). Spinel possesses dentate grain boundaries to margarite and chlorite (Fig. 2c, 2d), and thus shows to be overgrown by those minerals. Contrasting that, spinel grain boundaries to calcite are always straight.

Hoegbomite has a distinct yellow-brown to dark brown pleochroism and sometimes shows lamellar twinning. It is always closely associated with green spinel, either as a corona or as tabular crystals along the margins (Fig. 2a). The grain boundaries between the two minerals are always sharp. Large, homogeneous hoegbomite crystals usually contain tiny grains of spinel (Fig. 3). These textures clearly demonstrate that hoegbomite formed at the expense of spinel. Similar replacement textures have been described by Watson (1925), Friedman (1952), Woodford and Wilson (1976) and by Zakrzewski (1977). Hoegbomite is also found at spinel-magnetite grain boundaries (Fig. 2a), a feature previously observed by Leake and Skirrow (1960) and Coolen (1981).

Corundum contains considerable amounts of iron (up to 1 wt% measured as FeO), but no titanium ($TiO_2 < 0.03$ wt%). It is always closely associated with anhedral to vermicular *magnetite* (Fig. 2b, 2d). This assemblage clearly replaces spinel, forming coronae or pseudomorphs. In the latter, relics of green spinel can often be recognized (Fig. 2b). From the textural relationships it is not clear

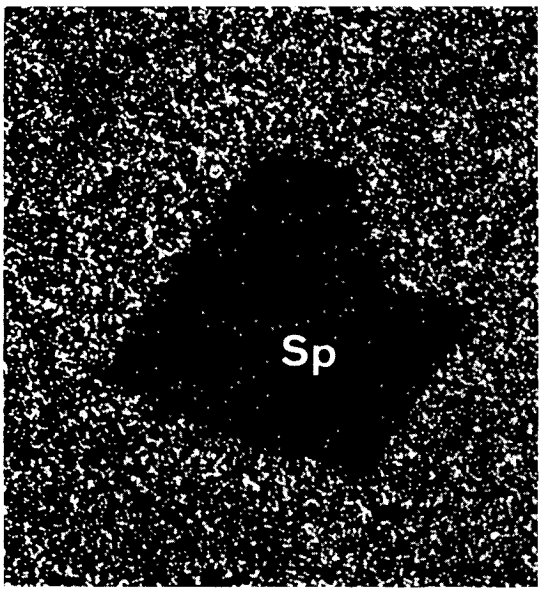

Fig. 3. Ti-Kα scanning picture of hoegbomite with an inclusion of spinel (Sp). Largest diameter of spinel is 0.05 mm

Table 3. Electron microprobe analyses of main minerals (tr = concentration close to detection limit)

wt%	Margarite (10 analyses)		Chlorite (10 analyses)		Phlogopite (12 analyses)		Anorthite (12 analyses)	
	mean	s.dev	mean	s.dev	mean	s.dev	mean	s.dev
Al_2O_3	50.5	0.5	24.8	0.4	21.3	0.6	36.6	0.3
TiO_2	0.04	0.03	0.03	0.03	0.55	0.09	tr	
SiO_2	30.8	0.4	26.3	0.6	35.8	0.2	43.8	0.3
MgO	0.15	0.05	24.0	2.6	17.3	0.9	<0.02	
CaO	12.2	0.5	<0.2		tr		20.2	0.2
MnO	tr		0.10	0.10	<0.06		<0.04	
FeO[a]	0.44	0.10	12.3	3.0	9.5	0.8	0.11	0.04
Na_2O	0.97	0.18	<0.02		0.14	0.02	0.16	0.09
K_2O	0.17	0.14	0.02	0.03	10.17	0.06	0.01	0.01
F	tr		tr		0.3	0.1	<0.09	
Cl	0.01	0.01	0.01	0.01	0.01	0.00	0.01	0.00
H_2O calc	4.55		12.20		3.92		–	
Total[b]	99.8		99.8		99.0		100.9	

Numbers of ions on the basis of:

	7 cations	10 cations	8 cations	8 oxygens
Al	3.93	2.87	1.85	1.98
Ti	0.00	0.00	0.03	0.00
Si	2.03	2.59	2.64	2.01
Mg	0.01	3.52	1.90	0.00
Ca	0.86	0.00	0.00	0.99
Mn	0.00	0.01	0.00	0.00
Fe^{2+}	0.02	1.01	0.59	0.00
Na	0.12	0.00	0.02	0.01
K	0.01	0.00	0.96	0.00
F	0.00	0.00	0.07	0.00
Cl	0.00	0.00	0.00	0.00
OH	2.00	8.00	1.93	–

[a] total Fe as FeO
[b] wt% H_2O calculated assuming perfect stoichiometry

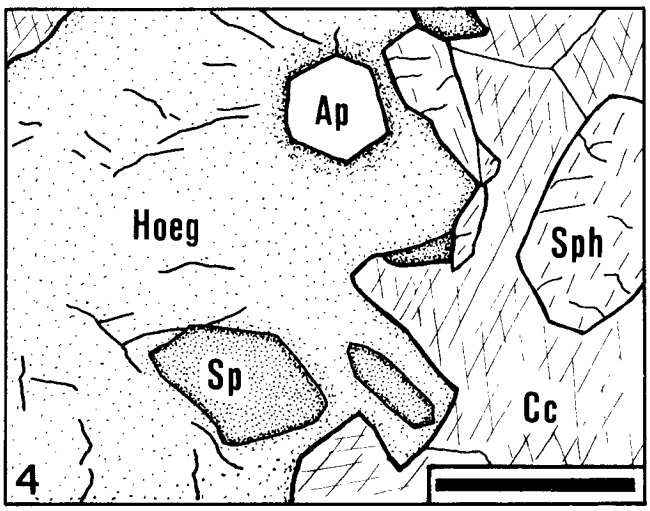

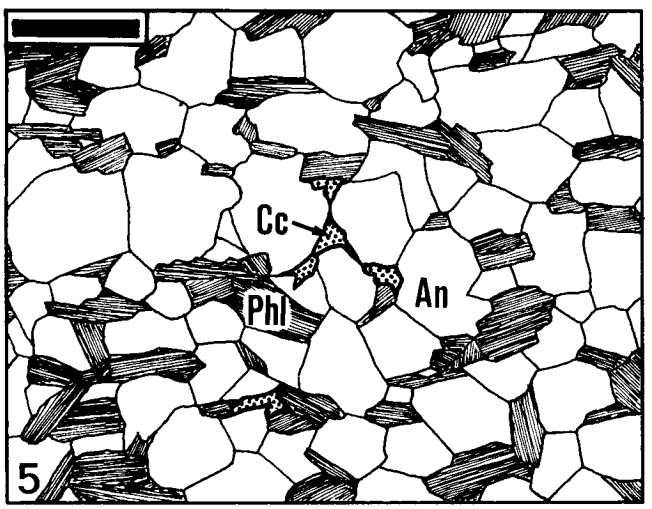

Fig. 4. Hoegbomite (Hoeg) with inclusions of idiomorphic apatite (Ap) and spinel (Sp). *Cc* = calcite, *Sph* = sphene. Drawing from thin section. Bar is 0.1 mm

Fig. 5. Relics of calcite (Cc) in the anorthite (An)-phlogopite(Phl)-matrix, which shows a granoblastic-polygonal texture. Drawing from thin section. Bar is 0.2 mm

whether formation of hoegbomite or of corundum + magnetite was the first stage of spinel alteration. Both reactions seem to have occurred contemporaneously.

Margarite is present as brownish flakes which overgrow spinel (Fig. 2c) as well as hoegbomite and corundum (Fig. 2d). Thus, formation of margarite post-dates the spinel alterations mentioned above. The Ti-bearing margarite with appreciable amounts of Na substituting for Ca (up to 1.2 wt% Na_2O) contains minor quantities of Cl and traces of F (Table 3).

Pale green *chlorite* of ripidolite composition (Table 3) overgrows spinel (Fig. 2d), hoegbomite and corundum (Fig. 2b, 2d). It also replaces margarite which can be observed as relics within large chlorite flakes (Fig. 2b, 2d). Chlorite therefore represents the final alteration product of spinel. Sometimes spinel relics are not recognized anymore, and the calcite lenses consist of margarite, chlorite and calcite only.

Idiomorphic *fluor-apatite* with SO_4^{2-} partially replacing PO_4^{3-} (S measured as SO_3^{2-} up to 1.16 wt%) contains 2.1 to 2.7 wt% F and minor amounts of Cl (up to 0.04 wt%). Usually it is closely associated with hoegbomite, sometimes as idiomorphic inclusions (Fig. 4), and found only within the calcite lenses. La and Ce could not be detected by microprobe ($La_2O_3 < 0.06$ wt%, $Ce_2O_3 <$ 0.06 wt%).

Matrix

The groundmass around the calcite lenses is characterized by a granoblastic-polygonal texture consisting of fresh *anorthite* with near-endmember composition (Table 3) and brownish green *phlogopite* (Fig. 5). The Ti-bearing phlogopite contains an average of 0.3 wt% F and minor amounts of Cl (Table 3). In the matrix, calcite is found only as interstitial relics (Fig. 5), while it shows a perfect mosaic texture inside the calcite lenses.

The accessory *clinozoisite* grains very often possess a brownish core of *allanite* which produces a pleochroic halo in co-existing phlogopite. The clinozoisite rims around allanite are free of REE. They are significantly richer in epidote component than the REE-free clinozoisite from the calcite lenses (Table 4), which is enclosed by spinel and probably represents an earlier generation. The composition of the allanite cores is given in Table 7.

Ilmenite is the main opaque accessory mineral in the rock. It has average MnO-contents of 2.1 wt% and is often rimmed by rutile or sphene. *Zircon* was also found in the anorthite-phlogopite-matrix. It is dominantly $ZrSiO_4$ with small amounts of U, Hf, Y and Dy.

Table 4. Electron microprobe analyses of clinozoisite (tr = concentration close to detection limit). Clinozoisite from the matrix surrounds allanite, clinozoisite from the lenses is enclosed by spinel

	Clinozoisite from matrix (6 analyses)		Clinozoisite from lenses (4 analyses)	
wt%	mean	s.dev	mean	s.dev
Al_2O_3	27.6	0.5	29.4	0.9
TiO_2	0.08	0.03	0.03	0.02
SiO_2	39.0	0.5	38.3	0.6
MgO	0.06	0.04	0.8	0.9
CaO	24.2	0.2	23.5	0.8
MnO	< 0.04		< 0.04	
Fe_2O_3[a]	7.7	0.3	5.7	0.4
Na_2O	tr		tr	
K_2O	0.03	0.01	< 0.01	
F	< 0.09		tr	
Cl	0.01	0.01	0.01	0.01
H_2O calc	1.94		1.94	
Total[b]	100.6		99.7	
Numbers of ions on the basis of 8 cations:				
Al	2.52		2.68	
Ti	0.00		0.00	
Si	3.02		2.96	
Mg	0.01		0.09	
Ca	2.01		1.94	
Mn	0.00		0.00	
Fe^{3+}	0.45		0.33	
Na	0.00		0.00	
K	0.00		0.00	
F	0.00		0.00	
Cl	0.00		0.00	
OH	1.00		1.00	
Fe/(Fe + Al)	0.15		0.11	

[a] total Fe as Fe_2O_3

[b] REE below microprobe detection limit (see Table 1), wt% H_2O calculated assuming perfect stoichiometry

Table 5. Electron microprobe analyses of spinel and associated hoegbomite (5 individual pairs and mean of 29 pairs, tr = concentration close to detection limit). ΔM^{4+} and ΔM^{2+} are absolute changes in cation contents per unit subcell of 8 oxygens for the reaction spinel → hoegbomite (see text)

wt%	1		2		3		4		5		Sp (29 analyses)		Hoeg (29 analyses)	
	Sp	Hoeg	Sp	Hoeg	Sp	Hoeg	Sp	Hoeg	Sp	Hoeg	mean	s.dev	mean	s.dev
Al_2O_3	60.7	60.2	61.0	61.6	61.1	60.8	58.3	59.5	60.5	61.1	60.6	1.8	60.9	1.6
TiO_2	<0.03	3.90	0.03	4.64	<0.03	3.89	0.03	4.30	<0.03	4.51	tr		4.01	0.86
MgO	11.79	9.29	11.65	9.80	11.92	9.46	10.77	9.38	8.61	6.86	10.25	1.6	8.44	1.15
CaO	<0.01	<0.01	<0.01	<0.01	<0.01	<0.01	0.02	<0.01	0.06	0.05	0.05	0.07	0.04	0.07
MnO	<0.40	<0.40	0.63	<0.40	<0.40	<0.40	<0.40	<0.40	0.87	<0.40	0.22	0.33	tr	
FeO	24.6	23.0	23.9	21.9	24.5	22.0	26.4	23.0	27.0	23.4	25.0	1.9	22.4	0.8
ZnO	1.58	0.87	1.59	0.88	1.69	0.96	1.58	0.90	2.25	1.17	2.12	0.81	1.09	0.16
Total[a]	98.7	97.3	98.8	98.8	99.2	97.1	97.1	97.1	99.3	97.1	98.2		96.9	
Numbers of cations on the basis of 8 oxygens:														
Al	3.90	3.89	3.91	3.89	3.91	3.91	3.86	3.86	3.94	3.96	3.94		3.94	
Ti	0.00	0.16	0.00	0.19	0.00	0.16	0.00	0.18	0.00	0.19	0.00		0.17	
Mg	0.96	0.76	0.95	0.78	0.96	0.77	0.90	0.77	0.71	0.56	0.84		0.69	
Ca	0.00	0.00	0.00	0.00	0.00	0.00	0.00	0.00	0.00	0.00	0.00		0.00	
Mn	0.00	0.00	0.03	0.00	0.00	0.00	0.00	0.00	0.04	0.00	0.01		0.00	
Fe^{2+}	1.02	0.94	1.00	0.87	1.02	0.91	1.10	0.92	1.19	1.04	1.09		0.97	
Fe^{3+}[b]	0.10	0.11	0.09	0.11	0.09	0.09	0.14	0.14	0.06	0.04	0.06		0.06	
Zn	0.06	0.04	0.06	0.04	0.07	0.04	0.07	0.04	0.09	0.05	0.09		0.04	
Σ(cations)	6.04	5.90	6.04	5.87	6.05	5.88	6.07	5.91	6.03	5.84	6.03		5.87	
ΔM^{4+}	0.16		0.19		0.16		0.18		0.19		0.17			
ΔM^{2+}	−0.30		−0.35		−0.33		−0.34		−0.38		−0.33			

[a] without H_2O, total Fe as FeO, $SiO_2 < 0.19$ wt%, $Cr_2O_3 < 0.02$ wt%, NiO < 0.36 wt%, $V_2O_5 < 0.19$ wt%
[b] Fe^{3+} calculated on the basis of $\Sigma M^{3+} = 4.00$

Accessory minerals occurring *in the calcite lenses as well as in the groundmass* are zirconolite, sphene, pyrite and chalcopyrite. In thin section the large, rounded grains of *zirconolite*[1] (maximum grain size observed is approximately 0.2 mm) are translucent reddish brown and anisotropic, the smaller ones are opaque. In reflected light it is similar to ilmenite. Where the zirconolite crystals are enclosed by phlogopite they are always surrounded by a broad pleochroic halo. Inclusions of zirconolite in phlogopite which has been partially replaced by chlorite show that formation of zirconolite preceeded the final stage of spinel alteration. Baddeleyite, commonly associated with zirconolite (Hussak and Prior 1897; Busche et al. 1972; Meyer and Boctor 1974; Zhuravleva et al. 1976; Williams 1978; Purtscheller and Tessadri 1985), was not found in the Bergell sample. *Sphene* is the most important REE-bearing mineral. It is idiomorphic or xenomorphic, and some of the larger grains exhibit lamellar twinning. *Pyrite* and *chalcopyrite* are less frequent in the groundmass than in the calcite lenses, where they are associated with magnetite and spinel. Usually chalcopyrite is enclosed by pyrite.

Mineral compositions

Hoegbomite

Electron microprobe analyses of the Bergell hoegbomites show relatively low oxide totals based on $Fe_{total} = FeO$ (Table 5). The deviation from 100 wt% does not disappear by calculating trivalent iron contents according to the simplified hoegbomite formula $M^{2+}_{2-2x}Ti_xM^{3+}_4O_8$ proposed by Zakrzewski (1977). Cr_2O_3, V_2O_5, NiO and SiO_2 have not been detected (see Table 5). Minor quantities of elements not analyzed might be present, since hoegbomite can contain considerable amounts of Co (Čech et al. 1976), Sn (Spry 1982) and Ga (Wilson 1977). Another possible explanation for the low oxide totals is the presence of additional components not detectable by microprobe, e.g. BeO and H_2O. Hoegbomite containing 0.10 wt% BeO has been described by Wilson (1977). The possible water content of hoegbomite is a matter of debate in literature. McKie (1964) considered the range of hoegbomite composition to be $M^{2+}_{1.0-1.6}Ti_{0.2-0.4}M^{3+}_{3.7-4.3}O_{7.6-8.0}(OH)_{0.0-0.4}$. Nel (1949) reported considerable OH^--contents, but stated that this may be due to chlorite contamination. Hoegbomite from the Liganga titanomagnetite ores in Tanzania does not contain any OH^- or H_2O, as demonstrated by infrared analyses (Zakrzewski 1977). In the Bergell hoegbomites however, an average of 0.02 OH^- per formula unit seems to be present, corresponding to 0.10 wt% OH^-. The amount of OH^- was calculated assuming charge-balance of the cation substitution effective during formation of hoegbomite from spinel (see below). The average composition of the Bergell hoegbomites thus is given by the formula

$$Fe^{2+}_{0.97}Mg_{0.69}Zn_{0.04}Ti_{0.17}Al_{3.94}Fe^{3+}_{0.06}O_{7.98}(OH)_{0.02}.$$

1) The polymorph was not determined by X-ray analysis and the name zirconolite is used here arbitrarily

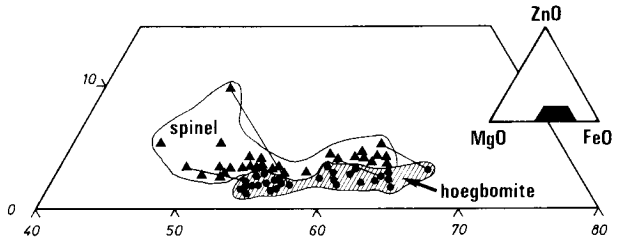

Fig. 6. Triangular plot ZnO-MgO-FeO showing the composition of spinel and hoegbomite (in mole %, total Fe as FeO). The tielines connect four pairs of spinel and associated hoegbomite. They demonstrate that relative to pre-existing spinel hoegbomite is richer in molar FeO, but poorer in molar ZnO

Electron microprobe analyses of spinel-hoegbomite-pairs are given in Table 5. The mean values of 29 pairs demonstrate that Al^{3+} and Fe^{3+}, calculated on the basis of $\Sigma M^{3+} = 4.00$ (Zakrzewski 1977), remained constant during formation of hoegbomite from spinel. Most individual pairs show the same relationship (e.g. pairs No. 3 and 4). Thus, the replacement of spinel by hoegbomite in the Bergell marble can be represented by the cation substitution $1.94(Mg^{2+}, Fe^{2+}, Zn^{2+}, Mn^{2+}, Ca^{2+}) \rightleftharpoons Ti^{4+}$, where average absolute $\Delta Mg^{2+} > \Delta Fe^{2+} > \Delta Zn^{2+} > \Delta Mn^{2+}$ (Table 5). To maintain charge-balance an average of 0.12 OH^- must be substituted along with Ti^{4+}. Table 5 and Figure 6 show that relative to pre-existing spinel the Bergell hoegbomites are richer in molar FeO, but poorer in molar ZnO. The relative enrichment in iron is consistent with the results from the study of Coolen (1981). The data for ZnO however, contrast the 1:1 distribution found by Coolen (1981). With very few exceptions the Mn-and Ca-contents are higher in spinel than in associated hoegbomite.

In another marble sample from Cima di Vazzeda, Zn-free spinel (ZnO < 0.48 wt%) was altered to Zn-free hoegbomite (Gieré 1984) with average cation contents of 5.54 per unit-subcell, showing that the composition of hoegbomite depends on the composition of pre-existing spinel. Similar compositional relationships between spinel and associated hoegbomite have previously been pointed out by Moleva and Myasnikov (1952), Zakrzewski (1977) and Coolen (1981).

Rutile and ilmenite are accessory constituents of many hoegbomite-assemblages and have been considered as a possible source for titanium (Christophe-Michel-Lévy and Sandréa 1953; Wilson 1977; Teale 1980; Coolen 1981; Essene et al. 1982; Ackermand et al. 1983; Angus and Middleton 1985).

In the Bergell marble rutile as well as ilmenite occur only in the matrix surrounding the hoegbomite-bearing calcite-lenses. Furthermore, neither sphene nor any other Ti-bearing minerals have been found as relics within hoegbomite or spinel, which is virtually Ti-free ($TiO_2 < 0.03$ wt%, see Table 5). These observations indicate a metasomatic origin of the titanium required for the production of hoegbomite. Friedman (1952) also explained formation of hoegbomite from spinel by titanium metasomatism.

Zirconolite

The zirconolite composition (Table 6) corresponds well to the generalized formula $(M_I)(M_{II})(M_{III})_2O_7$, where:

Table 6. Electron microprobe analyses of the Bergell zirconolites

wt%	Zirconolite				
	1	2	3	4	5
ZrO_2	34.5	34.4	35.2	34.7	35.0
CaO	13.37	13.39	12.04	13.34	12.75
TiO_2	38.3	39.0	36.0	38.5	37.3
Al_2O_3	0.68	0.64	0.83	0.67	0.82
Fe_2O_3[a]	4.4	4.0	5.9	4.4	5.2
MgO	0.01	0.01	0.01	0.03	0.04
ZnO	<0.04	<0.04	0.07	0.04	<0.04
SiO_2	0.17	0.17	0.13	0.15	0.17
ThO_2	0.41	0.45	1.02	0.57	1.03
La_2O_3	0.06	0.08	0.16	0.08	0.11
Ce_2O_3	1.03	1.01	1.47	0.89	1.41
Nd_2O_3	0.77	0.63	0.83	0.55	0.70
Gd_2O_3	0.26	0.23	0.42	0.23	0.30
Dy_2O_3	0.24	0.25	0.37	0.23	0.25
Y_2O_3	1.48	1.56	1.99	1.44	1.48
Total[b]	95.7	95.8	96.4	95.8	96.6
Numbers of cations on the basis of 7 oxygens:					
Zr	1.04	1.03	1.08	1.04	1.06
Ca	0.89	0.88	0.81	0.88	0.85
Ti	1.78	1.81	1.70	1.79	1.74
Al	0.05	0.05	0.06	0.05	0.06
Fe^{3+}	0.14	0.12	0.19	0.14	0.16
Mg	0.00	0.00	0.00	0.00	0.00
Zn	0.00	0.00	0.00	0.00	0.00
Si	0.01	0.01	0.01	0.01	0.01
Th	0.01	0.01	0.01	0.01	0.02
La	0.00	0.00	0.00	0.00	0.00
Ce	0.02	0.02	0.03	0.02	0.03
Nd	0.02	0.01	0.02	0.01	0.02
Gd	0.01	0.00	0.01	0.00	0.01
Dy	0.00	0.01	0.01	0.00	0.01
Y	0.05	0.05	0.07	0.05	0.05
Total	4.02	4.00	4.00	4.00	4.03
Ti/Zr	1.71	1.76	1.57	1.72	1.64

[a] total Fe as Fe_2O_3
[b] without UO_2, H_2O and traces of Nb and Sm
Ba and Ta not detected by wavelength spectrum analysis

$M_I = Ca^{2+}, Fe^{2+}, Mg^{2+}, Mn^{2+}, Zn^{2+}, Co^{2+}, Na^+, REE^{3+}, Y^{3+}$
$M_{II} = Zr^{4+}, U^{4+}, Th^{4+}, Pb^{2+}, REE^{3+}, Y^{3+}$
$M_{III} = Ti^{4+}, Zr^{4+}, Al^{3+}, Fe^{3+}, Cr^{3+}, Nb^{5+}, Ta^{5+}$

(Wark et al. 1974; Mazzi and Munno 1983). Although zirconolite was analyzed quantitatively for 15 elements, the oxide totals are relatively low, because the mineral has an extremely complex chemistry containing 30 or more elements with concentrations in excess of 0.1 wt% (Wark et al. 1974).

The M_I-site is nearly filled up by Ca, REE and Y, suggesting that most of the iron is present as Fe^{3+}. Fe-cation equivalents, therefore, have been listed as Fe^{3+} in Table 6. The amounts of Zr^{4+} and Th^{4+} are sufficient to fill completely the M_{II}-site. Excess Zr^{4+} shares the M_{III}-site with Ti^{4+}, Si^{4+}, Al^{3+} and Fe^{3+} (Gatehouse et al. 1981).

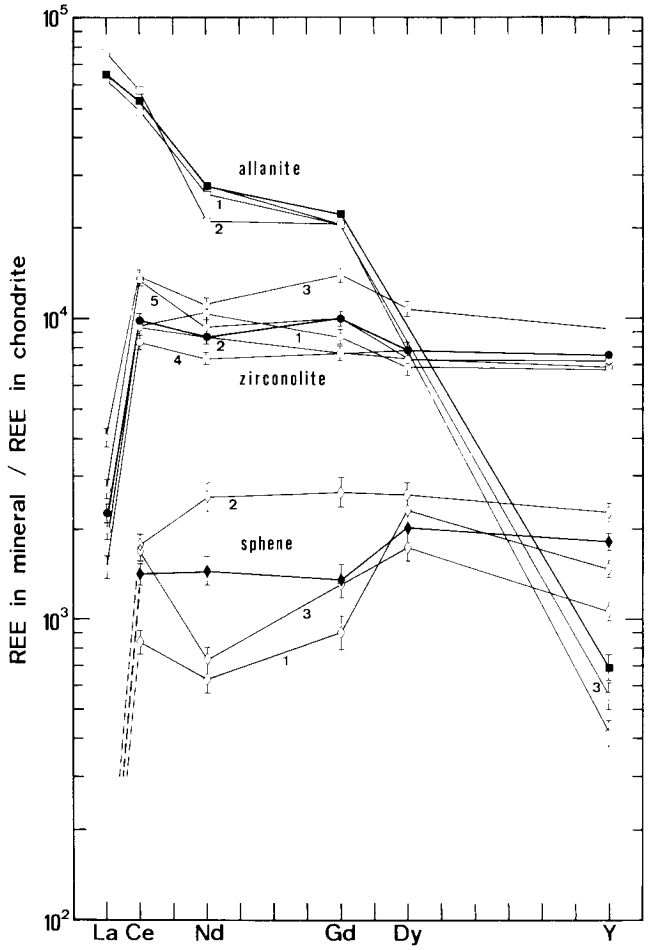

Fig. 7. Chondrite-normalized REE patterns of the Bergell zirconolite, allanite and sphene. The chondritic values are taken from Wakita et al. (1971). Numbers refer to the analyses in Tables 6 and 7. Open symbols are single analyses in different grains, full symbols are mean values (zirconolite and allanite: average of 10 analyses, sphene: average of 9 analyses). Error bars show the relative errors due to counting statistics (1 sigma). Points without error bars have errors smaller than symbol

Table 7. Electron microprobe analyses of the Bergell allanites and sphenes

wt%	Allanite			Sphene		
	1	2	3	1	2	3
ZrO_2	0.54	0.52	0.48	0.57	0.45	0.55
CaO	17.49	17.19	17.04	27.3	27.1	27.2
TiO_2	<0.15	<0.15	<0.15	36.7	35.8	37.0
Al_2O_3	23.06	23.53	24.84	1.47	1.90	1.53
Fe_2O_3[a]	10.8	8.4	8.3	–	–	–
FeO[b]	–	–	–	0.40	0.60	0.53
MgO	0.45	1.09	1.06	<0.01	<0.01	<0.01
ZnO	<0.03	<0.03	<0.03	tr	0.03	tr
SiO_2	35.80	35.68	35.77	30.66	30.22	30.46
ThO_2	0.49	0.61	0.32	0.03	0.03	0.04
La_2O_3	2.49	3.05	2.48	<0.01	<0.01	tr
Ce_2O_3	5.2	6.1	5.6	0.09	0.19	0.18
Nd_2O_3	1.94	1.58	2.04	0.05	0.19	0.05
Gd_2O_3	0.62	0.61	0.62	0.03	0.08	0.04
Dy_2O_3	<0.03	<0.03	<0.03	0.08	0.09	0.06
Y_2O_3	0.12	0.09	0.12	0.32	0.49	0.23
F	<0.27	<0.27	<0.27	<0.27	<0.27	<0.27
Cl	tr	tr	tr	tr	tr	tr
H_2O calc	1.77	1.77	1.79	–	–	–
Total[c]	100.8	100.2	100.5	97.7	97.2	97.9
Numbers of ions on the basis of:						
	8 cations			3 cations		
Zr	0.02	0.02	0.02	0.01	0.01	0.01
Ca	1.58	1.56	1.53	0.97	0.97	0.97
Ti	0.00	0.00	0.00	0.92	0.90	0.93
Al	2.30	2.35	2.46	0.06	0.08	0.06
Fe^{3+}	0.69	0.54	0.52	–	–	–
Fe^{2+}	–	–	–	0.01	0.02	0.01
Mg	0.06	0.14	0.13	0.00	0.00	0.00
Zn	0.00	0.00	0.00	0.00	0.00	0.00
Si	3.02	3.02	3.00	1.02	1.01	1.01
Th	0.01	0.01	0.01	0.00	0.00	0.00
La	0.08	0.10	0.08	0.00	0.00	0.00
Ce	0.16	0.19	0.17	0.00	0.00	0.00
Nd	0.06	0.05	0.06	0.00	0.00	0.00
Gd	0.02	0.02	0.02	0.00	0.00	0.00
Dy	0.00	0.00	0.00	0.00	0.00	0.00
Y	0.01	0.00	0.01	0.01	0.01	0.00
F	0.00	0.00	0.00	0.00	0.00	0.00
Cl	0.00	0.00	0.00	0.00	0.00	0.00
OH	1.00	1.00	1.00	–	–	–

[a] total Fe as Fe_2O_3
[b] total Fe as FeO
[c] wt% H_2O calculated assuming perfect stoichiometry

The Bergell zirconolites have high Ti/Zr-ratios (Table 6). This could be due to: 1) minor excess Zr^{4+}, which affects the Ti/Zr-ratio as a function of formation temperature (Wark et al. 1974; Gatehouse et al. 1981), 2) absence of Ta^{5+} and 3) very small contents of Nb^{5+}. Both, Ta^{5+} and Nb^{5+}, can substitute for Ti^{4+} in considerable amounts. In carbonatitic environments, zirconolite accommodates up to 2.9 wt% Ta_2O_5 and 30.2 wt% Nb_2O_5 into its structure (Zhuravleva et al. 1976).

U has not been determined quantitatively, but its presence was revealed by wavelength spectrum analysis. Together with U, the high Th-concentrations (Table 6) account for the zirconolite radioactivity which causes broad, intensely pleochroic haloes in surrounding phlogopite.

REE are present in concentrations up to 3.25 wt% (analysis 3, Table 6) with Ce and Nd always being the most abundant constituents (Tables 8 and 9). In addition to the REE listed in Table 8, trace amounts of Sm have been detected. Other REE have not been analyzed. The chondrite-normalized REE patterns of the Bergell zirconolites (chondritic values taken from Wakita et al. 1971) rise steeply from La to Ce and then remain virtually constant (Fig. 7). Zirconolites in altered pyroxenites (Borodin et al. 1956, 1961) exhibit more fractionated patterns with a strong enrichment in the light REE (LREE), particularly in Ce, Nd and Sm. In contrast to that, zirconolites in terrestrial and lunar igneous rocks (Busche et al. 1972; Lovering and Wark 1974; Meyer and Boctor 1974; Wark et al. 1974; Harding et al. 1982) as well as in the Oetztal metacarbonates (Purtscheller and Tessadri 1985) are enriched in the heavier REE. This variation in relative REE contents seems to reflect availability of REE during crystallization in the different

Table 8. REE- and Y-concentrations (wt%) in zirconolite, allanite and sphene (tr = concentration close to electron microprobe detection limit)

	Zirconolite (10 analyses)			Allanite (10 analyses)			Sphene (9 analyses)		
	mean	min.	max.	mean	min.	max.	mean	min.	max.
La_2O_3	0.09	0.06	0.16	2.59	1.93	4.94	tr		
Ce_2O_3	1.05	0.88	1.47	5.7	4.7	7.6	0.15	<0.03	0.25
Nd_2O_3	0.69	0.46	0.94	2.06	1.58	2.45	0.11	<0.03	0.23
Gd_2O_3	0.30	0.23	0.42	0.67	0.59	0.84	0.04	<0.02	0.13
Dy_2O_3	0.27	0.17	0.37	tr			0.07	<0.03	0.17
Y_2O_3	1.63	1.08	2.35	0.15	0.04	0.25	0.39	<0.02	1.05
Total	4.03			11.2			0.76		

environments. The general statement of Kochemasov (1980) that terrestrial zirconolites are enriched in LREE and those from the moon in heavy REE (HREE) cannot be confirmed.

Allanite

Allanite can be represented by the ideal formula $A_2M_3Si_3O_{12}(OH)$. The A-sites can be occupied by Ca^{2+}, Sr^{2+}, Mn^{2+}, REE^{3+}, Y^{3+} and Th^{4+}, the M-sites by Al^{3+}, Fe^{3+}, Fe^{2+}, Mn^{3+}, Mn^{2+}, Mg^{2+}, Zn^{2+}, Ti^{4+} and Zr^{4+} (Deer et al. 1962; Dollase 1971). The Bergell allanites are rich in ZrO_2 (average $ZrO_2 = 0.51$ wt%, maximum $ZrO_2 = 0.58$ wt%) and MgO (average MgO = 0.86 wt%, maximum MgO = 1.34 wt%). In addition to the elements listed in Table 7, traces of Ba, Mn and Sm have been detected by wavelength spectrum analysis. Some allanites contain Dy in concentrations close to microprobe detection limit (see Table 1).

Average REE and Y contents as well as their range are given in Table 8. Ce is always the most abundant REE, followed by La and Nd. The values of relative REE and Y abundances (Table 9) are very similar to those found in metasomatic allanites from limestone skarns of southern Siberia (Rudashevskiy 1969) and from carbonate veins in the Mountain Pass district, California (Murata et al. 1957), except that the Bergell allanites are richer in Gd. The chondrite-normalized REE patterns of the Bergell allanites exhibit a strong enrichment in LREE and a characteristically low slope between Nd and Gd (Fig. 7). Similar LREE fractionation is shown by igneous, metamorphic and hydrothermal allanites (Exley 1980; Brooks et al. 1981; Harding et al. 1982; see also Deer et al. 1962).

Sphene

Electron microprobe analyses of sphene are given in Table 7. All analyzed sphenes are rich in ZrO_2 (average $ZrO_2 = 0.50$ wt%). Similarly high ZrO_2-contents are reported by Staatz et al. (1977) for sphenes from a thorite vein in Idaho and from Alaskan syenites.

Sphene has much lower REE and Y contents than the other two REE-minerals (Table 8), but because it is much more abundant it may contain the major part of the REE in the rock. There is a wide variation in the REE patterns of different grains (Fig. 7). All analyzed sphenes lack detectable La, a few sphenes however contain La_2O_3 in concentrations close to microprobe detection limit (e.g. analysis 3, Table 7). Fleischer and Altschuler (1969) and Fleischer (1978) showed that the geological environment has an important effect on the relative concentrations of lanthanides and Y in igneous sphene. Sphenes from alkaline and granitic rocks are enriched in LREE (Dodge and Mays 1972; Cullers and Medaris 1977; Staatz et al. 1977; Exley 1980, Henderson 1980), while those crystallizing at high pressures in trondhjemites exhibit a strong enrichment in the middle REE (Hellman and Green 1979). Staatz et al. (1977) reported that sphenes occurring in a thorite vein from Idaho contain practically no LREE, but considerable amounts of Gd, Dy, Er, Yb and Y. By comparison with samples from alkaline rocks they concluded that REE and some minor elements such as Zr and Th are accommodated into the structure without appreciable fractionation. The quantities of REE and Zr then, may reflect availability of those particular elements during formation of sphene in the Bergell marble.

Table 9. Average relative amounts of REE and Y in zirconolite, allanite and sphene ($REE_2O_3 + Y_2O_3 = 100\%$)

	Zirconolite	Allanite	Sphene
La_2O_3	2.3	23.3	0.0
Ce_2O_3	26.1	50.9	19.7
Nd_2O_3	17.0	18.5	13.9
Gd_2O_3	7.4	6.0	5.7
Dy_2O_3	6.8	0.0	9.6
Y_2O_3	40.4	1.3	51.1

Discussion

The textural relationships indicate replacement of a spinel-calcite-marble by anorthite + phlogopite. Metasomatism is clearly demonstrated by the stepwise alteration of spinel to 1) hoegbomite or corundum + magnetite, 2) margarite and 3) chlorite. The anorthite-phlogopite-matrix formed prior to chloritization, together with zirconolite and probably the other REE-bearing accessory phases allanite and sphene. This implies the introduction of Ti, Zr, REE, Y, Nb, U and Th by the metasomatic fluid during the first two steps of spinel alteration.

Mobility of these same elements has been inferred to have occurred under a wide variety of conditions (p, T, fluid composition and salinity): during allanite formation in limestone skarns (Rudashevskiy 1969; Pavelescu and Pa-

velescu 1972), hedenbergite-ilvaite skarn formation (Salemink 1985), metasomatic alteration of Ta-bearing iron ores (Zhuravleva et al. 1976), fenitization of quartzites (Martin et al. 1978), granite alteration (Alderton et al. 1980 [tourmalinization]), hydrothermal alteration of tholeiitic flood basalts (Hellman et al. 1979 [Maddina volcanics, Australia]) and during formation of hydrothermal veins (Rekharskiy and Rekharskaya 1969; Staatz et al. 1977 [thorite vein, Idaho], Van Wambeke 1977).

These examples demonstrate that under certain conditions high valence cations such as Ti^{4+}, Zr^{4+}, Nb^{5+}, Ta^{5+}, U^{4+}, Th^{4+} and Y^{3+} are transported together with REE, suggesting a common transport mechanism (see also Bandurkin 1961).

In hydrothermal systems REE are assumed to migrate as complexes (e.g. Kosterin 1959; Ganeyev 1962; Mineyev 1963; Balashov and Krigman 1975). Experimental investigations on water-rich vapors, however, indicate very slight partitioning of REE into the H_2O vapor relative to silicate minerals and rhyolitic liquid at low total pressures (Cullers et al. 1973; Mysen 1979). Flynn and Burnham (1978) found that relative to pure water, the presence of Cl^- and F^- increased the vapor/silicate-melt partitioning of REE. They showed that while the vapor/melt partition coefficient very much favored the silicate-melt, it increased with increasing vapor chloride molality suggesting the formation of Cl^--complexes by the REE under magmatic conditions (granitic melt, $T = 800°$ C, $p = 1.25$ kb and 4.0 kb). Their results indicated also that CO_2 was not an effective complexing agent for REE at 800° C and 4 kb, in agreement with the study of Zielinski and Frey (1974). Contrasting that, Wendlandt and Harrison (1979), working in the system K_2O-Al_2O_3-SiO_2-CO_2, found the REE to be strongly enriched in the CO_2 vapor relative to the alkalic silicate-melt at low pressures.

The experimental investigations cited above indicate that: 1) a H_2O-rich fluid probably was unable to transport REE under the p-T-conditions found in the eastern Bergell contact aureole ($p = 3$ kb, $T > 520°$ C, see Trommsdorff and Evans 1980) and 2) CO_2 probably was not an effective complexing agent, because a CO_2-rich fluid is unlikely to have been enriched in REE relative to the calc-alkaline melt from which the Bergell intrusives derive.

Cl^--complexes are improbable as well, because all the hydrous minerals contain only very small amounts of Cl (max. Cl in apatite is 0.04 wt%, for other minerals see Tables 3, 4 and 7). The close association of fluor-apatite ($F =$ 2.1 to 2.7 wt%) with hoegbomite, as well as the contemporaneous formation of abundant F^--bearing phlogopite ($F =$ 0.3 wt%) and REE-bearing minerals suggest that F^- was the most likely ligand. The possibility of complexing REE and other high valence cations with fluorine under hydrothermal conditions was previously pointed out by Bandurkin (1961), Mineyev (1963), Balashov and Krigman (1975) and by Alderton et al. (1980).

The examples mentioned above show also, that in many cases potassium as well as phosphorus are transported along with high valence cations and REE, suggesting two additional transport mechanisms, possibly effective in hydrothermal systems:

1. Potassium might form polynuclear complexes with the high valence cations and/or the REE in a similar way as demonstrated for Al^{3+} and Si^{4+} by Anderson and Burnham (1983) in their study on feldspar solubility.

2. Phosphorus might form PO_4^{3-}-complexes with the high valence cations and/or the REE (see also Mineyev 1963; Kapustin 1966).

The possibility of transporting REE and other high valence cations as K^+- or PO_4^{3-}-complexes is supported by petrographic observations at different localities: in the Bergell marble zirconolite, and probably allanite and sphene also, formed contemporaneously with the anorthite-phlogopite-matrix; further, fluor-apatite is usually idiomorphic and closely associated with hoegbomite. Fenitization of country rocks around nepheline syenites of the Lovozero massif, Kola peninsula, caused formation of zirkelite, rosenbuschite and sphene in association with biotite and apatite (Semenov et al. 1963). In metasomatic tetraphlogopite-calcite-rocks, Zhuravleva et al. (1976) found hatchettolite, pyrochlore, zirkelite and baddeleyite always in contact with apatite. Moleva and Myasnikov (1952) described zincian hoegbomite-gahnite-apatite-assemblages from veins in a chlorite rock. In contact metamorphic dolomitic marbles of the eastern Bergell, fluorine-bearing titanian clinohumite is usually associated with idiomorphic fluor-apatite (Gieré, in prep.). In the Malenco serpentinites, northern Italy, Trommsdorff and Evans (1980) described veins containing titanian hydroxyl-clinohumite, perovskite and hydroxyl-apatite.

In these assemblages the formation of minerals which incorporate REE and the other high valence cations might have been caused by crystallization of phlogopite and/or apatite. This hypothesis could explain also the apatite inclusions in the Bergell hoegbomite (Fig. 4).

The veins from Val Malenco however, demonstrate that the transport of titanium is not restricted to fluids rich in potassium or fluorine.

Furthermore, Mineyev (1963) found no significant correlation between K_2O and REE in metasomatic rocks associated with albite-riebeckite-granites from Kasakhstan, but a direct linear correlation between Na_2O, F and yttrian earths, which he explained by formation of polynuclear complexes of the $NaYF_6$-type.

Conclusions

The following conclusions can be drawn from this study:

1. At the contact to the Bergell calc-alkaline intrusives, a spinel-calcite-marble has been partially replaced by anorthite + phlogopite. Spinel was metasomatically altered in three subsequent steps to 1) hoegbomite or corundum + magnetite, 2) margarite and 3) chlorite. Replacement of spinel by hoegbomite can be described by the substitution

$$1.94(Mg^{2+}, Fe^{2+}, Zn^{2+}, Mn^{2+}, Ca^{2+}) \rightleftharpoons Ti^{4+} + 0.12(OH^-).$$

The hoegbomite composition is dependant on the composition of pre-existing spinel.

2. The anorthite-phlogopite-matrix formed prior to chloritization, at the same time as zirconolite and probably allanite and sphene. Potassium thus was introduced into the marble along with REE and other high valence cations possibly as polynuclear complexes. The most likely ligands are F^- and PO_4^{3-}, as indicated by the presence of abundant fluorine-bearing phlogopite and fluor-apatite. Crystallization of apatite and phlogopite might have caused formation of hoegbomite, zirconolite, allanite and sphene.

3. Allanite exhibits typical REE patterns with enrichment in the LREE. The REE-concentrations in zirconolite and sphene seem to reflect availability of a specific REE during their formation.

Acknowledgements. The author would like to thank Prof. V. Trommsdorff, Prof. B.R. Frost and Dr. R.D. Vocke, Jr. for their critical reviews of the manuscript. I also express my sincere gratitude to Dr. J. Sommerauer and P. Ulmer for assistance at the microprobe. The support of the Schweizerischer Nationalfonds (No. 2.601-0.85) is gratefully acknowledged.

References

Ackermand D, Windley BF, Herd RK (1983) Magnesian hoegbomite in a sapphirine-bearing rock from the Fiskenaesset region, W. Greenland. Mineral Mag 47:555–561

Alderton DHM, Pearce JA, Potts PJ (1980) Rare earth element mobility during granite alteration: Evidence from south-west England. Earth Planet Sci Lett 49:149–165

Anderson GM, Burnham CW (1983) Feldspar solubility and the transport of aluminium under metamorphic conditions. Am J Sci 283-A:283–297

Angus NS, Middleton R (1985) Compositional variation in hoegbomites from north Connemara, Ireland. Mineral Mag 49:649–654

Balashov YUA, Krigman LD (1975) The effects of alkalinity and volatiles on rare-earth separation in magmatic systems. Geochem Int 12/6:165–170

Bandurkin GA (1961) Behavior of the rare earths in fluorine-bearing media. Geochem Int 2:159–167

Blake GS, Smith GFH (1913) On varieties of Zirkelite from Ceylon. Mineral Mag 16:309–316

Borodin LS, Nazarenko II, Rikhter TL (1956) The new mineral zirconolite – a complex oxide of the AB_3O_7 type. Dokl Akad Nauk SSSR 110:845–848

Borodin LS, Bykova AB, Kapitonova TA, Pyatenko YUA (1961) New data on zirconolite and its niobium variety. Dokl Akad Nauk SSSR 134:1022–1024

Brooks CK, Henderson P, Rønsbo JG (1981) Rare-earth partition between allanite and glass in the obsidian of Sandy Braes, Northern Ireland. Mineral Mag 44:157–160

Bucher-Nurminen K (1981) The formation of metasomatic reaction veins in dolomitic marble roof pendants in the Bergell intrusion (Province Sondrio, Northern Italy). Am J Sci 281:1197–1222

Busche FD, Prinz M, Keil K, Kurat G (1972) Lunar zirkelite: a uranium-bearing phase. Earth Planet Sci Lett 14:313–321

Čech F, Rieder M, Vrána S (1976) Cobaltoan hoegbomite from Zambia. N Jahrb Mineral Mh 12:525–531

Christophe-Michel-Lévy M, Sandréa A (1953) La hoegbomite de Frain (Tchécoslovaquie). Bull Soc Franc Minéral Cristallogr 76:430–433

Coolen JM (1981) Hoegbomite and aluminium spinel from some metamorphic rocks and Fe-Ti-ores. N Jahrb Mineral Mh 8:374–384

Coughanour LW, Roth RS, Marzullo S, Sennett FE (1955) Solid-State Reactions and Dielectric Properties in the Systems Magnesia-Zirconia-Titania and Lime-Zirconia-Titania. J Res Natl Bureau of Standards 54/4:191–199

Cullers RL, Medaris LG, Haskin LA (1973) Experimental studies of the distribution of rare earths as trace elements among silicate minerals and liquids and water. Geochim Cosmochim Acta 37:1499–1512

Cullers RL, Medaris Jr LG (1977) Rare earth elements in carbonatite and cogenetic alkaline rocks. Examples from Seabrook Lake and Callander Bay, Ontario. Contrib Mineral Petrol 65:143–153

Deer WA, Howie RA, Zussman J (1962) Rock-forming minerals. Vol. 1, Longmans (London), Wiley (New York), pp 211–220

De Lapparent J (1946) Composition minéralogique, structure et origine des émeris de Turquie. Comptes Rend Acad Sci 223:227–228

Diethelm K (1984) Geologie und Petrographie des Bergell-Ostrandes II. Diplomarbeit ETH Zürich (unpublished)

Dodge FCW, Mays RE (1972) Rare earth element fractionation in accessory minerals, central Sierra Nevada batholith. US Geol Surv Prof Pap 800-D:D165–D168

Dollase WM (1971) Refinement of the crystal structures of epidote, allanite and hancockite. Am Mineral 56:447–464

Duggan MB (1976) Primary allanite in vitrophyric rhyolites from the Tweed Shield Volcano, north-eastern New Southwales. Mineral Mag 40:652–653

Essene EJ, Petersen EU, Peacor DR (1982) Nigerite-hoegbomite-spinel assemblages from Manitouwadge, Ontario and their significance. Am Geophys Union Trans 63:456 (abstract)

Evans BW (1964) Fractionation of elements in the pelitic hornfelses of Cashel-Lough Wheelaun intrusion, Connemara, Eire. Geochim Cosmochim Acta 28:127–156

Exley RA (1980) Microprobe studies of REE-rich accessory minerals: implications for Skye granite petrogenesis and REE mobility in hydrothermal systems. Earth Planet Sci Lett 48:97–110

Fleischer M (1978) Relation of the relative concentrations of lanthanides in titanite to type of host rocks. Am Mineral 63:869–873

Fleischer M, Altschuler ZS (1969) The relationship of the rare-earth composition of minerals to geological environment. Geochim Cosmochim Acta 33:725–732

Flynn RT, Burnham CW (1978) An experimental determination of rare earth partition coefficients between a chloride containing vapor phase and silicate melts. Geochim Cosmochim Acta 42:685–701

Friedman GM (1952) Study of hoegbomite. Am Mineral 37:600–608

Ganeyev IG (1962) On the possible transport of matter in the form of complicated complex compounds. Geochem Int 10:1042–1049

Gatehouse BM, Grey IE, Roderick JH, Rossel HJ (1981) Zirconolite, $CaZr_xTi_{3-x}O_7$: Structure Refinements for Near-End-Member Compositions with $x=0.85$ and 1.30. Acta Crystal B37:306–312

Gavelin A (1916) Ueber Hoegbomit. Ein neues gesteinbildendes Mineral aus dem Ruoutevarre-Gebiet in Lappland. Bull Geol Inst Uppsala 15:289–316

Gieré R (1984) Geologie und Petrographie des Bergell-Ostrandes I. Diplomarbeit ETH Zürich (unpublished)

Gieré R (1985) Metasedimente der Suretta-Decke am Ost- und Südostrand der Bergeller Intrusion: Lithostratigraphische Korrelation und Metamorphose. Schweiz Mineral Petrogr Mitt 65:57–78

Gillson JL, Kania JEA (1930) Emery deposits near Peekskill, N.Y. Econ Geol 25:506–527

Harding RR, Merriman RJ, Nancarrow PHA (1982) A note on the occurrence of chevkinite, allanite, and zirkelite on St. Kilda, Scotland. Mineral Mag 46:445–448

Hellman PL, Green TH (1979) The role of sphene as an accessory phase in the high-pressure partial melting of hydrous mafic compositions. Earth Planet Sci Lett 42:191–201

Hellman PL, Smith RE, Henderson P (1979) The Mobility of Rare Earth Elements: Evidence and Implications From Selected Terrains Affected by Burial Metamorphism. Contrib Mineral Petrol 71:23–44

Henderson P (1980) Rare Earth Element Partition Between Sphene, Apatite and Other Coexisting Minerals of the Kangerdlugssuaq Intrusion, E. Greenland. Contrib Mineral Petrol 72:81–85

Hussak E, Prior GT (1897) Lewisite and Zirkelite, two new Brazilian Minerals. Mineral Mag 11:80–88

Kapustin YUL (1966) Geochemistry of Rare-Earth Elements in Carbonatites. Geochem Int 3:1054–1064

Kochemasov GG (1980) Characteristics of the chemical composition of zirkelite from the moon and from the earth. Mineralogicheskij zurnal 2/6:30–39 (in russian)

Kosterin AV (1959) The possible modes of transport for the rare earths by hydrothermal solutions. Geochem Int 4:381–387
Leake BE (1965) A cordierite-rich magnetite-hoegbomite-orthopyroxene hornfels from Currywongaun, Connemara, Ireland. Am Mineral 50:1092–1095
Leake BE, Skirrow G (1960) The pelitic hornfelses of Cashel-Lough Wheelaun intrusion, County Galway, Eire. J Geol 68:23–40
Lovering JF, Wark DA (1974) Rare Earth Element Fractionation in Phases Cristallizing from Lunar Late-stage Magmatic Liquids. Lunar Sci V/2:445–446. Lunar Sci Inst, Houston
Mancktelow NS (1981) Hoegbomite of unusual composition from Reedy Creek, South Australia. Mineral Mag 44:91–94
Martin RF, Whitley JE, Woolley AR (1978) An Investigation of Rare-Earth Mobility: Fenitized Quartzites, Borralan Complex, N.W. Scotland. Contrib Mineral Petrol 66:69–73
Mazzi F, Munno R (1983) Calciobetafite (new mineral of the pyrochlore group) and related minerals from Campi Flegrei, Italy. Crystal structures of polymignyte and zirkelite: comparison with pyrochlore and zirconolite. Am Mineral 68:262–276
McKie D (1964) The hoegbomite polytypes. Mineral Mag 33:563–580
Meyer OA, Boctor NZ (1974) Opaque mineralogy: Apollo 17, rock 75035. Proc Fifth Lunar Sci Conf, Geochim Cosmochim Acta Suppl 5/1:707–716
Mineyev DA (1963) Geochemical differentiation of the rare-earths. Geochem Int 12:1129–1149
Moleva VA, Myasnikov VS (1952) On hoegbomite and its variety zinc-hoegbomite. Dokl Akad Nauk SSSR 83/5:733–736 (in russian)
Murata KJ, Rose Jr HJ, Carron MK, Glass JJ (1957) Systematic variation of REE in cerium-earth minerals. Geochim Cosmochim Acta 11:141–161
Mysen BO (1979) Trace-element partitioning between garnet peridotite minerals and water-rich vapor: experimental data from 5 to 30 kbar. Am Mineral 64:274–287
Nel HJ (1949) Hoegbomite from the corundum fields of eastern Transvaal. S Africa Geol Surv Mem 43:1–7
Oenay TS (1949) Ueber die Smirgelgesteine SW-Anatoliens. Schweiz Mineral Petrogr Mitt 29:357–491
Olson JC, Shawe DR, Pray LC, Sharp WN (1954) Rare-earth mineral deposits of the Mountain Pass district. San Bernardino County, California. US Geol Surv Prof Pap 261:1–76
Pavelescu L, Pavelescu M (1972) Study of Some Allanites and Monazites from the South Carpathians (Romania). Tscherm Mineral Petrogr Mitt 17:208–214
Purtscheller F, Tessadri R (1985) Zirconolite and baddeleyite from metacarbonates of the Oetztal-Stubai complex (northern Tyrol, Austria). Mineral Mag 49:523–529
Pyatenko YUA, Pudovkina ZV (1964) The lattice metric of $CaZrTi_2O_7$ crystals. Kristallografiya 9:98–100
Rekharskiy VI, Rekharskaya VM (1969) The new zirkelite-jordisite mineral paragenesis. Dokl Akad Nauk SSSR 184:144–147
Rossel HJ (1980) Zirconolite- a fluorite-related super-structure. Nature 283:282–283
Rudashevskiy NS (1969) Epidote-orthite from the metasomatites of southern Siberia. Vses Mineral Obshchest Zap 98/6:739–749 (in russian)
Salemink J (1985) Skarn and ore formation at Seriphos, Greece, as a consequence of granodiorite intrusion. Geologica Ultraiectina 40, PhD Univ Utrecht
Sargent KA (1964) Allanite in metamorphic rocks, Horn Area, Bighorn Mountains, Wyoming. Geol Soc Am Spec Pap 76:143
Semenov EI, Kochemasov GG, Bykova AV (1963) Zirkelite and rosenbuschite from contactmetasomatic rocks of the Lovozero massif. Trudy Inst Mineral, Geokhim i Kristallokhim Redkikh Elementov, Akad Nauk SSSR 15:106–109 (in russian)
Sinclair W, Eggleton RA (1982) Structure refinement of zirkelite from Kaiserstuhl, West Germany. Am Mineral 67:615–620
Spry PG (1982) An unusual gahnite-forming reaction, Geco base-metal deposit, Manitouwadge, Ontario. Canad Mineral 20:549–553
Staatz MH, Conklin NM, Brownfield IK (1977) Rare earths, thorium, and other minor elements in sphene from some plutonic rocks in west-central Alaska. J Res, US Geol Surv 5/5:623–628
Teale GS (1980) The occurrence of hoegbomite and taaffeite in a spinel-phlogopite schist from Mount Painter Province of South Australia. Mineral Mag 43:575–577
Trommsdorff V, Evans B (1979) Symposium on tectonic inclusions and associated rocks in serpentinites. Unpublished excursion guide to Alpe Albion, east of Bellinzona. Geneva, Sept 1979
Trommsdorff V, Evans B (1980) Titanian Hydroxyl-Clinohumite: Formation and Breakdown in Antigorite Rocks (Malenco, Italy). Contrib Mineral Petrol 72:229–242
Van Wambeke L (1977) The Karonge Rare Earth Deposit, Republic of Burundi: New Mineralogical-Geochemical Data and Origin of the Mineralization. Mineral Deposita 12:373–380
Wakita H, Rey P, Schmitt RA (1971) Abundances of the 14 rare-earth-elements and 12 other trace elements in Apollo 12 samples: five igneous and one breccia rocks and four soils. Proc 2nd Lunar Sci Conf, Geochim Cosmochim Acta Suppl 2:1319–1329
Wark DA, Reid AF, Lovering JF, El Goresy A (1974) Zirconolite (versus zirkelite) in lunar rocks. Lunar Sci IV:764–766. Lunar Sci Inst, Houston
Watson TL (1925) Hoegbomite from Virginia. Am Mineral 10:1–9
Wendlandt RF, Harrison WJ (1979) Rare Earth Partitioning Between Immiscible Carbonate and Silicate Liquids and CO_2 Vapor: Results and Implications for the Formation of Light Rare Earth-Enriched Rocks. Contrib Mineral Petrol 69:409–419
Williams CT (1978) Uranium-Enriched Minerals in Mesostasis Areas of the Rhum Layered Pluton. Contrib Mineral Petrol 66:29–39
Wilson AF (1977) A zincian hoegbomite and some other hoegbomites from the Strangeways Range, Central Australia. Mineral Mag 41:337–344
Woodford PJ, Wilson AF (1976) Sapphirine, hoegbomite, kornerupine, and surinamite from aluminous granulites, north-eastern Strangeways Range, central Australia. N Jahrb Mineral Mh 1:15–35
Zakrzewski MA (1977) Hoegbomite from the Fe-Ti deposit of Liganga (Tanzania). N Jahrb Mineral Mh 8:373–380
Zhuravleva LN, Berezina LA, Gulin YEN (1976) Geochemistry of Rare and Radioactive Elements in Apatite-Magnetite Ores in Alkali-Ultrabasic Complexes. Geochem Int 13/5:147–166
Zielinski RA, Frey FA (1974) An experimental study of the partitioning of a rare earth element (Gd) in the system diopside-aqueous vapor. Geochim Cosmochim Acta 38:545–565

Received December 16, 1986 / Accepted March 21, 1985